Porous silver nanosheets: a novel sensing material for nanoscale and microscale airflow sensors

2015 Nanotechnology 26 445501

(http://iopscience.iop.org/0957-4484/26/44/445501)

IOP Publishing Nanotechnology
Nanotechnology 26 (2015) 445501 (8pp) doi:10.1088/0957-4484/26/44/445501

Porous silver nanosheets: a novel sensing material for nanoscale and microscale airflow sensors

Ehsan Marzbanrad[1,2], Boxin Zhao[1,3] and Norman Y Zhou[1,2]

[1] Centre for Advanced Materials Joining, University of Waterloo, Waterloo, Canada
[2] Department of Mechanical and Mechatronics Engineering, University of Waterloo, Waterloo, Canada
[3] Department of Chemical Engineering, University of Waterloo, Waterloo, Canada

E-mail: nzhou@uwaterloo.ca

Received 4 May 2015, revised 25 August 2015
Accepted for publication 11 September 2015
Published 9 October 2015

Abstract

Fabrication of nanoscale and microscale machines and devices is one of the goals of nanotechnology. For this purpose, different materials, methods, and devices should be developed. Among them, various types of miniaturized sensors are required to build the nanoscale and microscale systems. In this research, we introduce a new nanoscale sensing material, silver nanosheets, for applications such as nanoscale and microscale gas flow sensors. The silver nanosheets were synthesized through the reduction of silver ions by ascorbic acid in the presence of poly(methacrylic acid) as a capping agent, followed by the growth of silver in the shape of hexagonal and triangular nanoplates, and self-assembly and nanojoining of these structural blocks. At the end of this process, the synthesized nanosheets were floated on the solution. Then, their electrical and thermal stability was demonstrated at 120 °C, and their atmospheric corrosion resistance was clarified at the same temperature range by thermogravimetric analysis. We employed the silver nanosheets in fabricating airflow sensors by scooping out the nanosheets by means of a sensor substrate, drying them at room temperature, and then annealing them at 300 °C for one hour. The fabricated sensors were tested for their ability to measure airflow in the range of 1 to 5 ml min^{-1}, which resulted in a linear response to the airflow with a response and recovery time around 2 s. Moreover, continuous dynamic testing demonstrated that the response of the sensors was stable and hence the sensors can be used for a long time without detectable drift in their response.

Keywords: nanosheet, nanosensor, anemometer, silver

1. Introduction

The rapid development of nanotechnology promises the existence of microscale and nanoscale machines in the not too distant future. Generally, the construction of a nanoscale or microscale system requires synthesis or fabrication of appropriately scaled structural blocks, a suitable energy source, a sound and economically feasible fabrication and assembly process, and adequate control and monitoring to help achieve these goals. Scientists can employ the numerous breakthroughs already made by the scientific and technological communities [27]. However, to reach the desired destination, a lot of work remains to be done. Nanosensors are crucial to these efforts. Employing nanomaterials for sensing has advantages because of the constructive effects of scaling down the sensing material to the nanoscale. Nanoparticles are being used to build a new generation of sensors with a wider sensitivity range than was achievable with large-scale sensing materials [8, 14, 19]. However, along with these new sensors, nanoscale and microscale systems also require the miniaturization of conventional sensors such as force, strain, weight and flow sensors. Among them, gas flow sensors are urgently needed for a wide range of applications—from nano- and micro-mechanical systems to medical apparatus and nano-bioassays [20]. Different types of large-scale sensors have been fabricated to measure gas flow, while the rapid

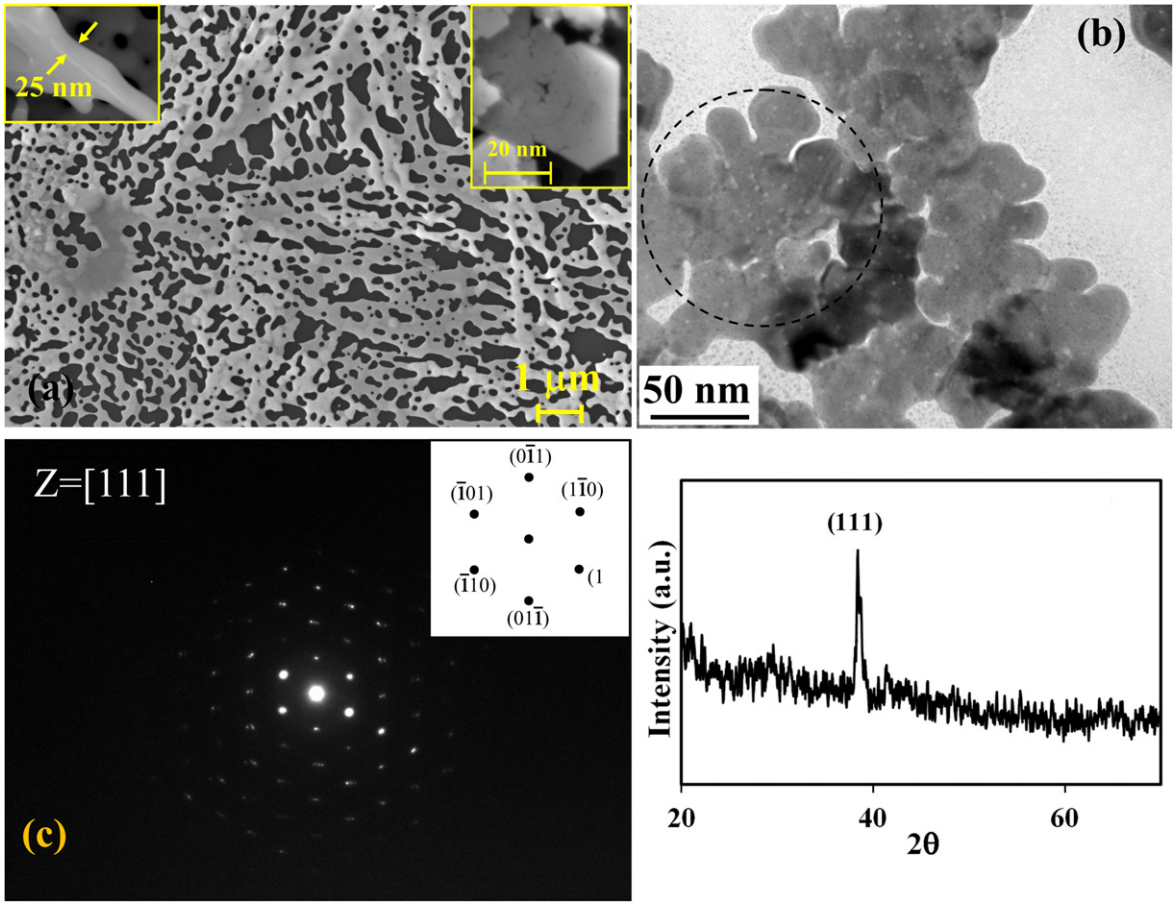

Figure 1. (a) SEM image of the synthesized silver nanosheet. The inset on the left demonstrates the thickness of the nanosheet, and the right inset image demonstrates a hexagonal structural block of the nanosheet. (b) TEM image of a nanosheet. (c) Selected area diffraction pattern of the marked area of 2(b). (d) x-ray diffraction pattern of the synthesized silver nanosheets.

development of micro- and nanoscale technologies is increasing the demand for miniaturized sensors [12]. Hot wire anemometers, currently available in macro scale, are one of the most common flow sensors. In a hot wire anemometer, the temperature and therefore electrical resistance of a metal wire is changed by gas flow. The convection heat transfer equation, the heat capacity of the sensing material, and the relationship between the temperature and electrical resistivity of the sensing material determine the sensor's sensitivity [10, 12]. Generally, increasing the surface area and decreasing the mass of the sensing material enhance the sensitivity of a sensor to an external stimulus. The thermal and electrical stability and mechanical strength of the sensing material are other parameters that must be considered in designing a reliable flow sensor. Hot wire anemometers have a wide range of applications, although they are not suitable for some conditions, such as high-vibration environments. In addition, fabricating micro- or nanoscale hot wire flow meters usually requires a very expensive apparatus [1, 3, 5, 6, 10, 13, 18, 21–23, 30]. Therefore, feasible new methods for the design and fabrication of accurate gas flow sensors for current and future applications are an important research topic.

One- and two-dimensional metallic nanoparticles can be considered as potential candidates for the sensing material of a hot wire flow meter. It has been reported that the electrical conductivity of the nanoparticles is decreased, and the temperature-dependence of their electrical conductivity is increased, by reducing the size of the nanoparticles [28]. Hence, metallic nanoparticles are a good candidate for sensing gas flow from the electrical property point of view. High specific surface area and acceptable mechanical strength are two other advantages of metallic nanoparticles for this application. On the other hand, thermal stability [9], electrical stability or electromigration resistance [24, 25] and high temperature corrosion [7] are important issues that must be considered in employing metallic nanoparticles as the sensing material of a flow sensor. Silver is a noble metal with excellent electrical and thermal conductivity, high mechanical strength and good corrosion resistance. In addition, silver nanoparticles have unique properties which have led to much research into this material. As a result of these studies, various silver nanoparticles with different sizes and morphologies have been synthesized [26, 29]. All of these facts, and the relatively low price of silver in comparison to alternatives such as gold and platinum, make it a promising choice for hot wire sensor fabrication.

We recently synthesized a new type of silver nanoparticle by the simultaneous self-assembly and nanojoining of

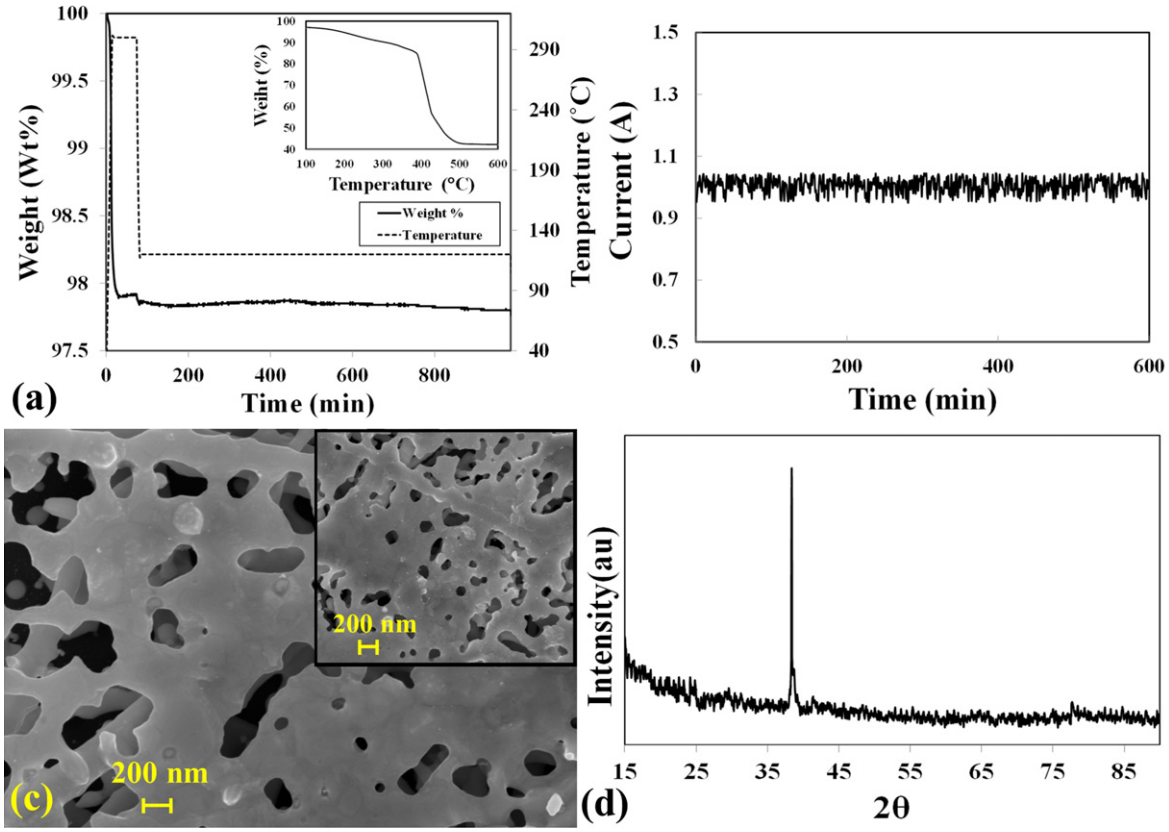

Figure 2. (a) TGA analysis of the silver nanosheet. Inset is the TGA curve of the PMAA. (b) Electrical current was passed through a silver nanosheet for 600 h, confirming the electrical stability of the sensing material. (c) SEM image of a silver nanosheet after annealing for 30 d at 150 °C. Inset demonstrates the nanosheet before annealing. (d) XRD pattern of the silver after annealing for 30 d at 150 °C.

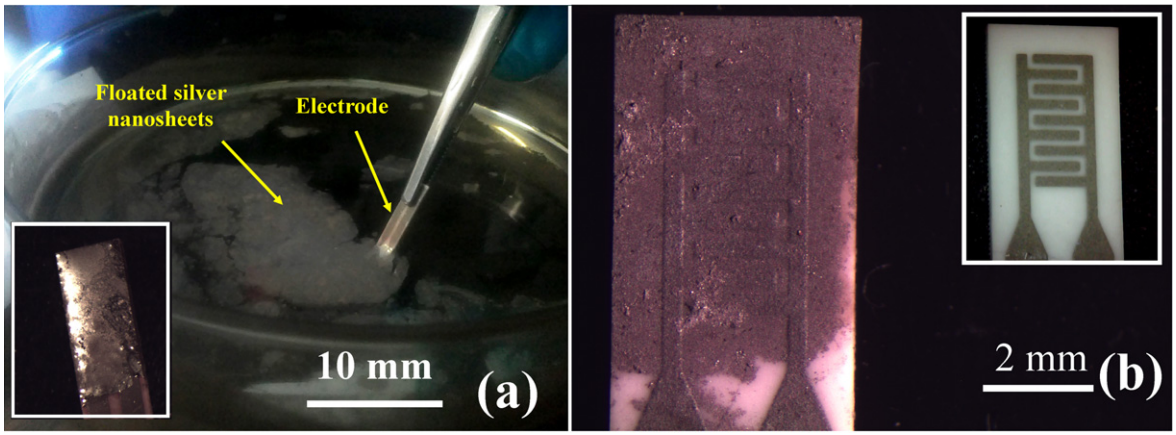

Figure 3. (a) Sensor fabrication by scooping. Inset shows deposited silver nanosheet immediately after scooping. (b) A silver nanosheet on the interdigitated electrodes. Inset is the interdigitated electrodes of the sensor substrate.

hexagonal and triangular silver nanoplates as structural blocks in the form of nanobelts, nanoflakes and porous nanosheets [15, 16]. Our synthesis is a fast, high-yield and feasible method. The thickness of these nanoparticles, including the nanosheets, is around 25 nm, and the nanosheets can be designed to be in the range of a few microns to a few millimeters in diameter. The boundaries between the structural blocks are perfect crystals; that is, they are defect free, which is important for good electrical conductivity [16]. Another important feature of this new type of silver nanoparticle is its unique surface texture [16]. The majority of the surface area of these nanoparticles is composed of a closed packed (111) crystal plane, which is the result of the realignment of the hexagonal and triangular nanoplates during the lateral nano-joining process. We have demonstrated by molecular dynamic simulation and experimental observation that the silver nanobelts are stable at high temperature and remain intact over a long period of annealing at high temperature because of their unique low energy surface texture [17]. We have used this new type of silver nanoparticles as filler

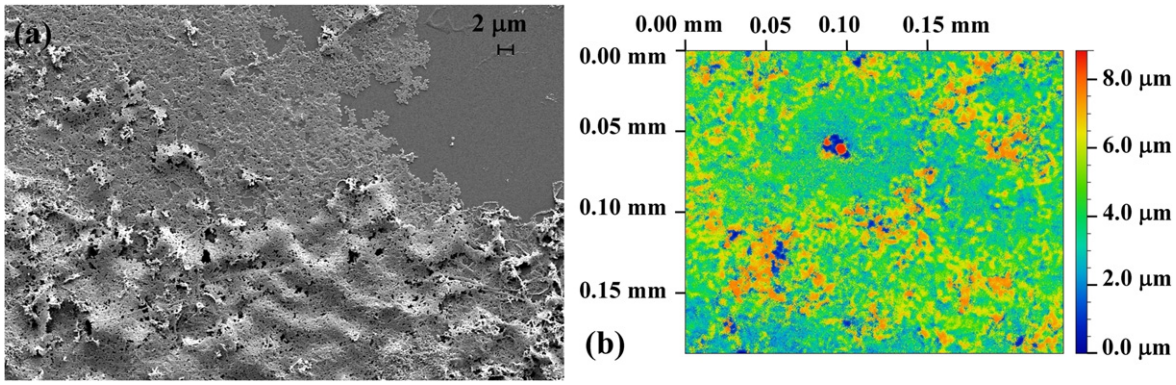

Figure 4. (a) SEM images of the scooped silver nanosheet on a silicon wafer; (b) roughness of the scooped silver nanosheet.

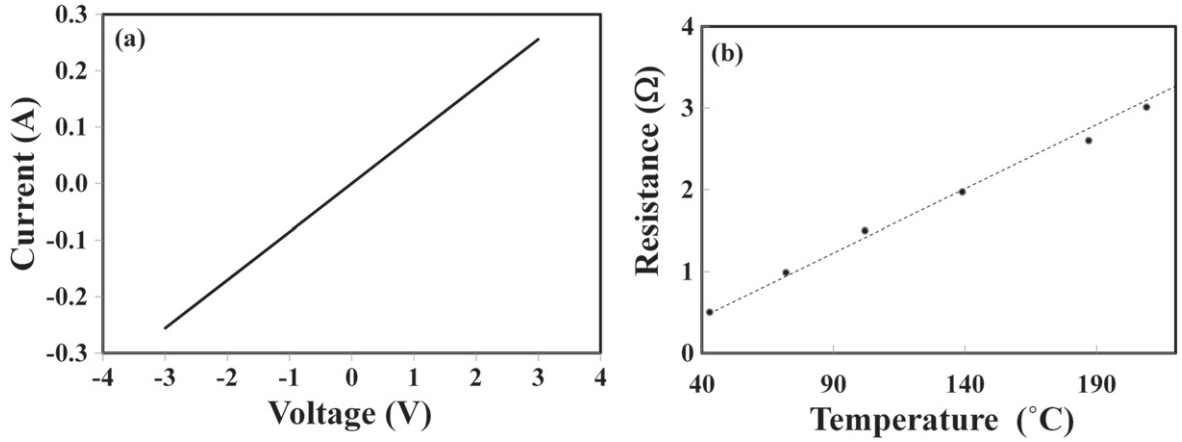

Figure 5. (a) *I–V* curve of a silver nanosheet; (b) the change of electrical resistance of a silver nanosheet versus temperature.

material to enhance the electrical conductive adhesive performance [2]. In the current research, we used silver nanosheets to fabricate a mass airflow sensor. The synthesis process, fabrication method, and response of the sensor will be discussed in this paper. Additionally, the results of a hot corrosion resistance investigation under atmospheric conditions, and observations of the electrical and thermal stability of the sensing material, are reported to address the essential requirements for a long-lasting sensor application.

2. Experimental procedure

2.1. Synthesis and characterization of the porous silver nanosheets

To synthesize silver nanosheets, 2.1 g of $AgNO_3$ (Sigma-Aldrich) was added to 60 ml of H_2O and shaken for one min to form a silver nitrate solution. A reducing solution was prepared separately by adding 0.68 g of ascorbic acid (Alfa Aesar) and 0.16 ml of poly(methacrylic acid, sodium salt) 40% in water (PMAA solution, Aldrich Chemistry, typical molecular weight 4000–6000) as a structure-directing reagent to 200 ml of H_2O. The mixture was then vigorously shaken for one min to dissolve the ascorbic acid. Synthesis was performed by adding the silver nitrate solution to the reducing solution. After a few seconds, the silver nanosheets self-assembled and floated on the solution.

Scanning and transmission electron microscopes (SEM and TEM) and optical profilometery were utilized to investigate the morphology and crystal structure of the synthesized nanosheets. To prepare SEM and optical profilometery samples, a silver nanosheet was put on a clean silicon wafer, then dried at 70 °C by using a hot plate and annealed at 300 °C for one h. For TEM observation, the nanosheet was put on a TEM grid, dried under standard room conditions, and then annealed at 300 °C for one hour.

An x-ray diffractometry (XRD) technique was utilized to characterize the crystal structure of the synthesized silver nanosheets. To prepare XRD samples, the floating nanosheets were collected using a filter paper (Whatman #1001042). The sample was dried at 70 °C, and then the nanosheets were detached by peeling away the filter paper and putting the sample on a piece of glass. XRD was performed using an x-ray tube with a wavelength output of Cu-Kα_1 ($\lambda = 0.154\,056$ nm).

The thermal stability of the silver nanosheets was investigated by annealing them at 150 °C for 100 h. The morphology and crystal structure of the silver nanosheets after annealing were investigated by SEM and XRD. The hot corrosion resistance of the nanosheets was investigated using a thermogravimetry machine under flow of air. The electrical

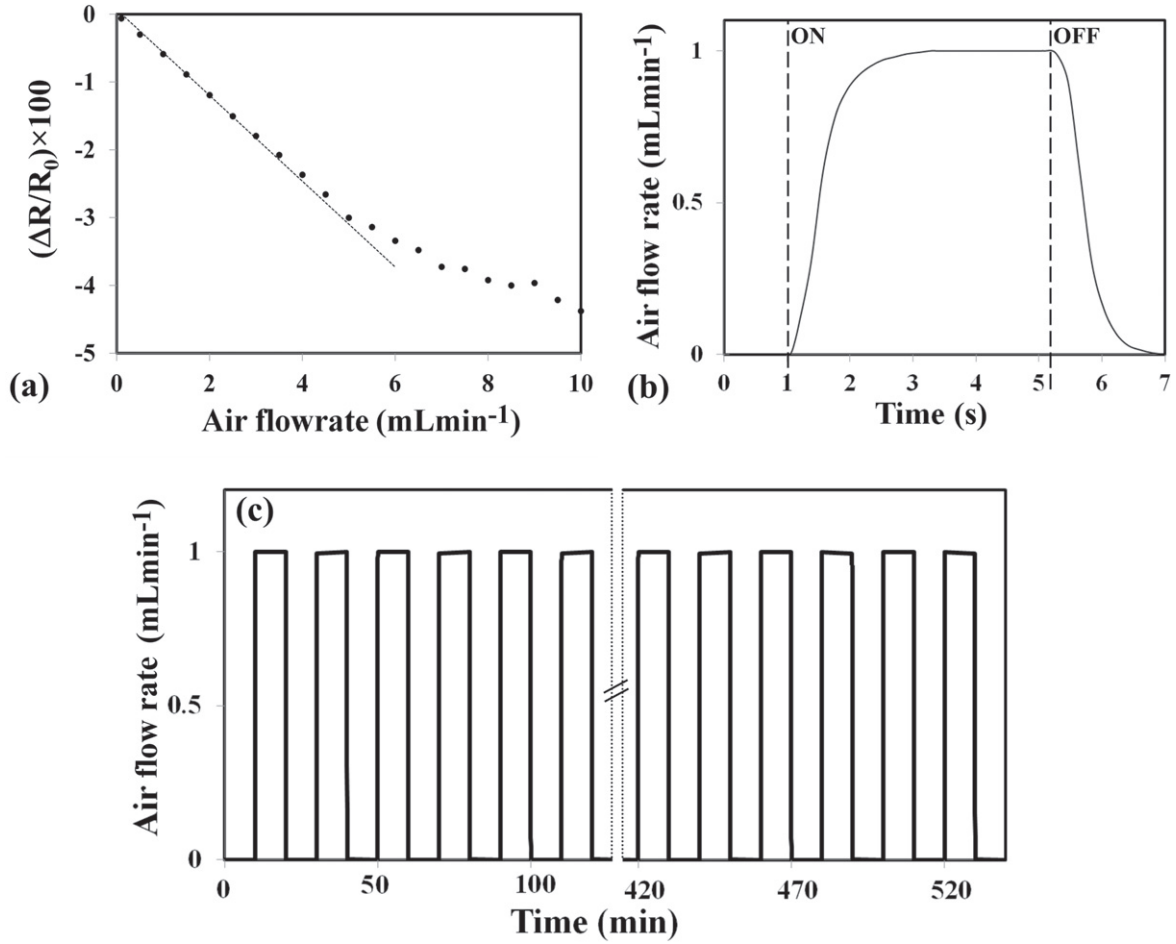

Figure 6. (a) The resistance change of the sensor versus the airflow rate. (b) Airflow versus time; the on and off times of the air solenoid valve are marked on the graph. (c) Dynamic test of the sensor; the duration of each on/off cycle was 20 min.

stability of the sensing material was evaluated by passing 982 mA through it for 500 h while the sensor was kept at 120 °C, which is its working temperature.

2.2. Sensor fabrication and test

An alumina substrate with interdigitated electrodes (spaced about 100 μm apart) was used for sensor fabrication. This substrate was equipped with a microheater on the back side of the electrodes. A nanosheet was loaded onto the electrodes by simply scooping it from the solution surface. To do that, the alumina substrate was dipped into the liquid and used to pick up a nanosheet in such a way that the sheet sat on the electrodes. After that, the sensor was dried at room temperature and then annealed at 300 °C for one h to remove the PMAA from the surface of the sheet. This sensor was installed in a chamber with a channel with a 1 mm^2 cross section. To examine the sensor, it was exposed to air flowing at different rates, and its electrical resistance was measured by a 16 bit data logger at a rate of 10 bits/s. A moving average noise rejection filtering with a window of 5 bits was used to smooth the data.

3. Results and discussion

3.1. Synthesis and characterization of sensing material

Figure 1(a) shows an SEM image of a nanosheet, revealing that the silver nanosheet is a continuous mesh of silver with irregularly shaped holes. The left inset of figure 1(a) is a high-magnification side view of a nanosheet clarifying that the thickness of the nanosheets is 25 nm. The TEM image of a sheet is presented in figure 1(b) and demonstrates that this sheet is composed of joined nanoplates. The selected area diffraction (SAD) pattern of the marked area of the TEM image is presented in figure 1(c). This SAD pattern confirms that the surface plane of the nanosheet is (111), although the structural blocks are not completely parallel. This tilt might have occurred during nanojoining, as predicted by molecular dynamic simulation [16]. The x-ray diffraction pattern of the nanosheets shows only one peak, belonging to the (111) crystal plane of silver (figure 1(d)), which confirms the structure of the nanosheets. These combined characterizations demonstrate that the synthesized silver nanosheet is a very thin sheet of silver, with a (111) surface crystal texture. Therefore, because of their low mass and high surface area, silver nanosheets are an excellent candidate for use as a

sensing material in hot wire anemometers. Moreover, the unique crystal structure and surface texture of the nanosheets could give this type of nanoparticle special properties, such as high stability, which may be beneficial for this application.

The synthesis mechanism for this type of nanoparticle was elucidated in [15, 16]. After the nucleation of initial silver clusters through reduction of silver ions by ascorbic acid, the PMAA covers (111) crystal planes of silver and controls the growth process to synthesize the hexagonal and triangular nanoplates. These nanoplates move randomly in the solution, and if they get close enough to each other they will join. In the case of silver nanosheets, we added silver nitrate solution to ascorbic acid. The reduction reaction happens immediately at the top layer of the reducing solution where silver ions exist, and the product floats on the reactor. The right inset of figure 1(a) is a high-magnification SEM image of a hexagonal structural block of the nanosheet, which is joined to the other structural blocks from one side. This SEM image verifies the proposed mechanism for the synthesis.

3.2. Stability of the silver nanosheets

The atmospheric corrosion resistance of the synthesized silver nanosheets was investigated using an annealing heat treatment with thermogravimetric analysis (TGA) at 120 °C under flow of air (figure 2(a)). For this experiment, first the sample was heated at 300 °C for one hour to remove the adsorbed PMAA molecules from the surface of the silver nanosheets. This happened successfully, which was evident by around 2% weight loss within the first 30 min of the TGA test. The Inset curve of figure 2(a) demonstrate the TGA test results of the PMAA, which shows the the PMAA decomposed in temperature range of 350 °C to 450 °C. It is well established that dicarboxylic acids tend to have all-trans conformation for the maximum number of bonds between carboxylate groups and silver nanoparticles [11]. Because of this, poly carboxylic acid chains such as PMMA likely exhibit trans-favoring conformations, which cause increased stress on the carbon chain backbone due to conformational entropy. This would be expected to catalyze degradation. Therefore, it can conclude that the observed weight loss in the TGA test of the silver nanosheets was happened because of the decomposition of the PMAA. After one hour annealing at 300 °C, the temperature was set at 120 °C and kept constant for 900 min. During this period, around 0.1% weight increase was observed, which was followed by the same amount of decrease in weight. Therefore, it can be concluded that no traceable oxidation occurred in the sample. Hence, silver nanosheets are not subject to oxidation when exposed to airflow at this temperature.

Electrical stability testing was performed on a silver nanosheet with current density equal to $1 \times 10\ \mathrm{A\,cm^{-2}}$, while its temperature was controlled at 120 °C. The current characteristic curve versus timing is demonstrated in figure 2(b). It is well known that electromigration causes a decreasing current regime versus time because of induced microstructural defects. However, in this case the current was stable over time, which suggests high electromigration resistance in the silver nanosheet. This result is compatible with the literature, where it has been reported that a thin film of silver with a high degree of (111)-orientation texture exhibits more electromigration resistance than one with a lower degree of (111)-orientation texture [4]. Moreover, it has been reported that pentagonal silver nanowires with (100) surface crystal are susceptible to electromigration at room temperature when a current density of $3.5 \times 10^7\ \mathrm{A\,cm^{-2}}$ is passed through a nanowire, and electromigration damage happens within a few hours [25]. Therefore, the (111) surface texture and defect-free boundary between the hexagonal and triangular structural blocks might result in high electromigration resistance, as observed in figure 2(b).

The structure and morphology of the silver nanosheets were observed after 30 days annealing at 120 °C, to scrutinize their response to temperature at the working temperature of the flow sensor, as thermal stability is one of the requirements for a durable and repeatable hot anemometer flow sensor. Figure 2(c) shows an SEM image of a silver nanosheet after annealing, confirming that the shape and morphology of the nanosheet kept its morphology intact during 30 days heat treatment. XRD analysis of heat treated silver nanosheets confirmed not only that the morphology, but also the crystal structure of the silver nanosheets was stable after heat treatment (figure 2(d)). This stability can be highlighted by comparison with that of silver pentagonal nanowires [9]. The silver nanowires degraded by annealing at 100 °C for 17 days while silver nanosheets are stable at this temperature [9]. The effect of the surface crystal texture of silver nanoparticles on their thermal stability was investigated, and it was clarified that the existence of low energy (111) crystal planes on the surface of nanocrystals leads to higher thermal stability [17]. In the case of silver nanosheets, the surface of the nanoparticles is almost all (111) plane and this special crystal structure results in superior thermal stability.

3.3. Sensor fabrication

A prototype sensor was fabricated by using an alumina sensor substrate to scoop out a floating silver nanosheet (figure 3(a)). Figure 3(b) illustrates the sensor fabricated on the alumina substrate, and the interdigitated electrodes of the sensor are shown in the inset. The existence of the PMAA layer on the surface of the silver nanosheets prevents direct contact between the nanosheets and reduces the electrical connection between the electrodes and the nanosheets. In addition, a PMAA layer may cause a small gap between silver islands and prevent complete nanojoining. TGA analysis of figure 2(a) revealed that the surface of the nanosheets can be cleaned by annealing at 300 °C. Therefore, the fabricated sensor was annealed at 300 °C for 1 h to remove the PMAA. After cleaning, adjacent silver nanosheets are capable of more spontaneous nanojoining, which can increase the conductivity of the layer. In addition, this heat treatment increases the electrical contact between the electrodes and the silver nanosheet by removing the PMAA surface layer.

Figure 3(b) shows that the deposited silver nanosheet is not flat. To clarify the morphology of the sensing layer,

deposition was done on the flat surface of a silicon wafer by scooping. The silicon wafer was selected for this observation to avoid complexity because of the roughness of the substrate. SEM observation demonstrated that the deposited layer was creased during scooping (figure 4(a)). Optical profilometry (3D universal profilometer, Rtec Instruments) was employed to examine the roughness of the deposited layer. Figure 4(b) shows an image prepared by optical profilometry. The colors represent the thickness of the nanosheet, and the color bar indicates the relation between color and thickness. Based on this measurement, the average roughness of the layer is 0.097 μm. The deposited layer creased because the solution trapped below the nanosheet layer during scooping (inset in figure 3(a)) evaporated, leading to shrinkage and crimping of the nanosheet.

3.4. Electrical properties of the fabricated sensor

Figure 5(a) demonstrates the *I–V* curve of the fabricated sensor. The linear relation between the applied voltage and the electric current passing through the silver nanosheets confirms the metallic nature of the silver nanosheet. The electrical resistance of the sensing material at different temperatures was measured under an inert atmosphere (figure 5(b)). This experiment revealed that the response of the sensor to temperature change is linear at a rate of 0.0157 $\Omega\,^{\circ}C^{-1}$ between 50 °C and 210 °C. This linear relation between the temperature change and the resistance of the sensor is important in reducing the complexity of the sensor response to airflow.

3.5. Sensor characterization

To investigate the response of the sensor to airflow, the sensor's temperature was kept at 120 °C using the micro heater. This enhanced the sensor's response to airflow by decreasing the initial conductivity of the sensing material. The resistance of the sensor in its flow chamber was measured at various flow rates in the range from 0.1 to 10 ml min^{-1} (figure 6(a)). This measurement clarified a linear relation between airflow and the resistance of the sheet, in the range of 0.1 to 5 ml min^{-1}. Therefore, a working range of 0.1 to 5 ml min^{-1} can be considered for this sensor and chamber geometry. A dynamic test was performed to find the response time of the sensor, which was around 2 s to respond to a 1 ml min^{-1} change in the flow (figure 6(b)). Finally, the repeatability of the sensor response was examined by a dynamic test for 560 min with an on-off cycle of 20 min (figure 6(c)), which revealed that the sensor is stable over a long dynamic experiment.

4. Conclusion

A high-aspect-ratio porous silver nanosheet was formed by simultaneous self-assembly and nanojoining of synthesized hexagonal and triangular silver nanoplates. The nanoplates resulted from the reduction of silver ions by ascorbic acid in the presence of PMAA molecules. The 25 nm-thick nanosheets will float on top of the reacting solutions after a few minutes. The atmospheric corrosion resistance, electrical or electromigration resistance, morphology, and crystal stability of the synthesized silver nanosheet were investigated. Observations revealed that the silver nanosheet has excellent stability at 120 °C from the oxidation, thermal and electrical points of view, which is essential for a durable flow sensor.

An alumina substrate with interdigitated electrodes was selected as a sensor baseplate. The sensor was fabricated by scooping out a piece of the floating silver nanosheets onto the electrodes. The nanosheet was fixed on the senor substrate by heat treatment for 1 h at 300 °C. This sensor was used to measure the flow rate of air. The sensor showed a linear response to airflow in the range of 0.1 to 5 ml min^{-1}. The response time of the sensor was around 2 s when the airflow changed by 1 ml min^{-1}. The dynamic test demonstrated that the response of the senor was stable after 9 h of continued dynamic on-off experiments. Therefore, it was concluded that the synthesized silver nanosheet is an excellent candidate for a hot wire flow sensor, having high stability, proper gain, a remarkable response time, and repeatability.

Acknowledgments

This work was supported by strategic research funds from the Natural Sciences and Engineering Research Council of Canada (NSERC).

References

[1] Adamec R J and Thiel D V 2010 Self heated thermo-resistive element hot wire anemometer *IEEE Sensors J.* **10** 847–8
[2] Amoli B M, Marzbanrad E, Hu A, Zhou Y N and Zhao B 2014 Electrical conductive adhesives enhanced with high aspect-ratio silver nanobelts *J. Macromol. Mater. Eng.* **229** 739–47
[3] Bensidhoum M T, Laghrouche M, Said A S, Montes L and Boussey J 2014 Fabrication flaws and reliability in MEMS thin film polycrystalline flow sensor *Microsyst. Technol.* **20** 1–7
[4] Bittner A, Seidel H and Schmid U 2011 Electromigration resistance and long term stability of textured silver thin films on LTCC *Microelectronic Eng.* **88** 127–30
[5] Buder U, Berns A, Petz R, Nitsche W and Obermeier E 2007 AeroMEMS wall hot-wire anemometer on polyimide substrate featuring top side or bottom side bondpads *IEEE Sensors J.* **7** 1095–101
[6] Dong X, Zhou Y, Zhou W, Cheng J and Su Z 2012 Compact anemometer using silver-coated fiber Bragg grating *IEEE Photonics J.* **4** 1381–6
[7] Elechiguerra J L, Larios-Lopez L, Liu C, Garcia-Gutierrez D, Camacho-Bragado A and Yacaman M J 2005 Corrosion at the nanoscale: the case of silver nanowires and nanoparticles *Chem. Mater.* **14** 6042–52
[8] Gon A W D V D, Smith R J, Gay J M, O'Connor D J and Veen J F V D 1990 Melting of Al surfaces *Surf. Sci.* **227** 143–9
[9] Khaligh H H and Goldthorpe I A 2013 Failure of silver nanowire transparent electrodes under current flow *Nanoscale Res. Lett.* **8** 235–41
[10] Kuo J T W, Yu L and Meng E 2012 Micromachined thermal flow sensors—a review *Micromachines* **3** 550–73

[11] Li Y and Wong C P 2006 Monolayer protection for electrochemical migration control in silver nanocomposite *Appl. Phys. Lett.* **89** 112112
[12] Liptak B G 2003 *Process Measurement and Analysis* (London: CRC Press)
[13] Liu H-B, Lin N, Pan S-S, Miao J and Norford L K 2013 High sensitivity, miniature, full 2D anemometer based on MEMS hot-film sensors *IEEE Sensors J.* **13** 1914–20
[14] Maruyama M 1989 Surface premelting phenomena of rare gas crystals *J. Cryst. Growth* **94** 757–61
[15] Marzbanrad E, Hu A, Zhao B and Zhou Y Effect of solution conditions on the fabrication of silver nanobelts, nanoflakes and porous nanosheets with (111) surface crystal orientation *In preparation*
[16] Marzbanrad E, Hu A, Zhao B and Zhou Y 2013 Room temperature nanojoining of triangular and hexagonal silver nanodisks *J. Phys. Chem.* C **117** 16665–76
[17] Marzbanrad E, Rivers G, Peng P, Zhao B and Zhou N Y 2015 How morphology and surface crystal texture affect thermal stability of a metallic nanoparticle: the case of silver nanobelts and pentagonal silver nanowires *Phys. Chem. Chem. Phys.* **17** 315–24
[18] Nagaiah N R, Sleiti A K, Rodriguez S, Kapat J S, An L and Chow L 2006 A novel design and analysis of a MEMS ceramic hot-wire anemometer for high temperature applications *J. Phys.: Conf. Ser.* **34** 277–82
[19] Nenow D 1984 Surface premelting *Prog. Cryst. Growth Charact.* **9** 185–225
[20] Nenow D and Trayanov A 1989 Surface premelting phenomena *Surf. Sci.* **213** 488–501
[21] Piotto M, Pennelli G and Bruschi P 2011 Fabrication and characterization of a directional anemometer based on a single chip MEMS flow sensor *Microelectron. Eng.* **88** 2214–7
[22] Sazhin O 2013 Novel mass air flow meter for automobile industry based on thermal flow microsensor I. Analytical model and microsensor *Flow Meas. Instrum.* **30** 60–5
[23] Sazhin O 2014 Novel mass air flow meter for automobile industry based on thermal flow microsensor II. Flow meter, test procedures and results *Flow Meas. Instrum.* **35** 48–54
[24] Song T-B, Chen Y, Chung C-H, Yang Y M, Bob B, Duan H-S, Li G, Tu K-N, Huang Y and Yang Y 2014 Nanoscale Joule heating and electromigration enhanced ripening of silver nanowire contacts *ACS Nano* **8** 2804–11
[25] Stahlmecke B, Heringdorf F-J M Z, Chelaru L I, Hoegen M H-V and Dumpich G 2006 Electromigration in self-organized single-crystalline silver nanowires *Appl. Phys. Lett.* **88** 053122
[26] Sun Y and Xia Y 2002 Shape-controlled synthesis of gold and silver nanoparticles *Science* **298** 2176–9
[27] Tang H, Chen J, Nie L, Kuang Y and Yao S 2007 A label-free electrochemical immunoassay for carcinoembryonic antigen (CEA) based on gold nanoparticles (AuNPs) and nonconductive polymer film *Biosens. Bioelectron.* **22** 1061–7
[28] Tanner D B and Larson D C 1968 Electrical resistivity of silver films *Phys. Rev.* **166** 652–5
[29] Tao A R, Habas S and Yang P 2008 Shape control of colloidal metal nanocrystals *Small* **4** 310–25
[30] Viard R, Talbi A, Merlen A, Pernod P, Frankiewicz C, Gerbedoen J-C and Preobrazhensky V 2013 A robust thermal microstructure for mass flow rate measurement in steady and unsteady flows *J. Micromech. Microeng.* **23** 065016